A Spectroscopic Approach to the Solvation of Anesthetics in Jets: Propofol(H2O)(n), n=4-6

ARTICLE *in* THE JOURNAL OF PHYSICAL CHEMISTRY A · AUGUST 2012

Impact Factor: 2.69 · DOI: 10.1021/jp305795u · Source: PubMed

THE JOURNAL OF PHYSICAL CHEMISTRY A

Article

pubs.acs.org/JPCA

A Spectroscopic Approach to the Solvation of Anesthetics in Jets: Propofol$(H_2O)_n$, $n = 4-6$

Iker León,[†] Emilio J. Cocinero,[†] Alberto Lesarri,[‡] Fernando Castaño,[†] and José A. Fernández*[,†]

[†]Departamento de Química Física, Facultad de Ciencia y Tecnología, Universidad del País Vasco—UPV/EHU, Barrio de Sarriena, s/n, 48940, Leioa, Spain

[‡]Departamento de Química Física y Química Inorgánica, Facultad de Ciencias, Universidad de Valladolid, E-47011 Valladolid, Spain

Supporting Information

ABSTRACT: Propofol is a widely used nonvolatile anesthetic that exerts its action by docking to $GABA_A$ receptors. The docking process is a competition between solvation of the anesthetic by the extracellular medium and the stabilization inside the active site, and therefore a deep knowledge of the process requires of a good understanding of the solvation process. In this work we create propofol−water complexes containing up to six water molecules using supersonic expansions. We determine their structure by means of a number of mass-resolved laser-based excitation spectroscopic techniques, namely two-color REMPI, UV/UV, and IR/UV double resonance techniques, combined with computational chemistry. The results clearly show that water tends to self-aggregate, interacting with the hydrophilic side of propofol. Furthermore, a transition from planar to three-dimensional structures is observed in propofol$(H_2O)_6$. Comparison with structural data from similar systems such as phenol−water and pure water clusters follows.

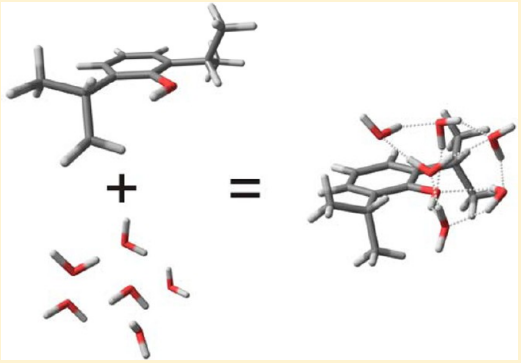

INTRODUCTION

It is well-known that, in biology, structure and function are intimately connected.[1] Most of the chemical processes that take place inside a cell are based on a key−lock type of interaction, guided by noncovalent forces.[2] However, such weak interactions are difficult to characterize due to their subtle contribution to the overall system energy.[2] Certainly, study of noncovalently bound systems in solution or in solids is hampered by the interaction with the surroundings, which largely perturbs the system and adds an important entropic contribution, making it impossible to extract other but average properties. A successful strategy for the investigation of weakly bound noncovalent systems is the combination of mass-resolved electronic and infrared spectroscopy in jets with quantum mechanical calculations.[3] Indeed, mass-resolved spectroscopy is a powerful tool to unravel the structure of molecules and their aggregates, especially when performed in supersonic expansions, where the cold rotational (a few kelvin) and vibrational (∼100 K), isolated environment allows exploring their conformational preferences without perturbation of their (vibrorotational) energy levels. However, the structures of the isolated molecules detected in the expansions cannot always be extrapolated to solution, due to the effect that the interaction with the liquid medium has on the gas phase structures. Fortunately, it is possible to fill this gap between gas phase and solution by studying the microsolvated species produced during the expansion, adding water molecules to the mixture in a controlled way. Building such a bridge between gas phase and solution with mass- and conformer-selective techniques is an important task in the study of molecules with biological activity, such as peptides,[4,5] sugars,[6,7] DNA bases,[8,9] or pharmaceuticals.[10,11]

Propofol (Scheme 1) is a broadly used general anesthetic. Based on structural considerations, the molecule presents five distinct conformers arising from the concerted large-amplitude motions of the isopropyl and hydroxy groups (Figure S1, Supporting Information). Gas phase microwave[12] and electronic spectroscopies[13,14] have proved that four conformations are stable in supersonic expansions, and their structures have been fully characterized. Introduction of a single water molecule results in reduction in the number of detected isomers to three, while a further reduction in the number of isomers to only two is observed in propofol$(H_2O)_{2,3}$.[15] Furthermore, only species based on the most stable propofol

Scheme 1. Propofol (2,6-Diisopropylphenol)

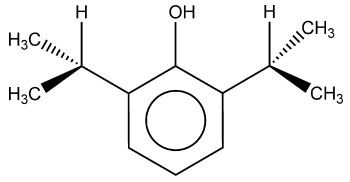

Received: June 13, 2012
Revised: July 17, 2012
Published: August 3, 2012

conformation are detected for such stoichiometries, and therefore, they mostly differ in the position of the water molecules, which form cyclic structures. Thus, previous studies demonstrate that one of the main consequences of solvation is the reduction in the number of conformations available for propofol, due to the energetic penalty experimented by those conformers in which the isopropyl groups induce larger steric hindrances.

Combining mass-resolved laser spectroscopic techniques with computational chemistry, we address here the question of what kind of structural changes are induced on the bare molecule by the successive addition of four to six water molecules.

Studies on the solvation of benzene[3,16] and phenol[17−21] with up to 12 water molecules have been previously reported. The main difference with the present system is the number of conformations that propofol itself, the chromophore, can adopt, which largely complicates the conformational landscape. Furthermore, while the interaction site with water was clear in phenol and benzene, it is hard to anticipate a priori the interaction geometry in propofol: the hydroxy group of phenol is clearly accessible for water to solvate, while in benzene, only the electronic π cloud can yield (weak) hydrogen bonds with the water molecules. However, propofol's hydroxy group is flanked by two bulky hydrophobic isopropyl groups, which impose serious steric hindrances for solvation, as demonstrated in previous studies.[13,14] Therefore, there is a competition for the water molecules between the aromatic ring and the hydroxy group. Thus comparison between the results from this work and those on phenol/water and benzene/water clusters will allow evaluating the influence of the hydrophobic effect in the solvation of propofol.

METHODS

Experimental Section. A detailed description of the experimental setup can be found elsewhere.[10,13] Propofol (97%, Sigma-Aldrich) was seeded at room temperature in He, Ne, or Ar without further modifications, and the mixture was expanded inside the chamber of a linear time-of-flight (Jordan Inc.) mass spectrometer. Water was added in a controlled way to optimize the signal from the clusters of the desired stoichiometry. Typical backing pressures of 1−2 bar were employed before the expansion, while the chamber of the mass spectrometer was kept at 10^{-5} mbar during operation.

The supersonic beam was skimmed before entering the ionization region of the mass spectrometer, where the molecules were interrogated with a variety of UV and IR laser-based spectroscopic techniques, namely two-color REMPI, UV/UV hole burning, and IR/UV hole burning.[11]

Theoretical Section. A first extensive exploration of the conformational landscape was achieved using a fast molecular mechanics method (MMFFs)[14] without imposing any geometric restriction to the systems. The structures were generated through advanced search algorithms that consist of a combination of the Monte Carlo procedures and "large scales low mode" (which uses frequency modes to create new structures). A minimum of 100 000 runs were performed for each stoichiometry, resulting in at least 25 000 structures (most of them redundant) in a 25 kJ/mol energy window. Such structures were grouped in families attending to their structural similarities. The most relevant (most stable) structures and representative structures of each family were further reoptimized at M06-2X/6-311++G(d,p).[15,16] While the molecular mechanics search was conducted with Macromodel,[22] ab initio calculations were performed with the Gaussian 09 suite of programs[23] on an Itanium- and Xeon-based cluster with 870 processors, available in the university's computer center, and on the cluster of the i2BASQUE foundation. Due to the flatness of the potential energy surface, a large number of iterations are required for each optimization. All the energy values presented in this work are zero point energy corrected. Binding energy values include also the Boys and Bernardi[24] counterpoise correction to the basis set superposition error. All optimizations were conducted imposing no structural constraints, and a normal-mode analysis was carried out to test for the absence of negative frequencies.

Calculated structures are named as W*n*S*m*, where n = 4−6 refers to the number of water molecules that form the cluster and m = 1 ,2, ... refers to the energetic order, starting with m = 1 for the global minimum.

RESULTS AND DISCUSSION

Figure 1 shows the two-color REMPI spectra of propofol-$(H_2O)_{0-6}$. The asterisks in Figure 1 indicate the position of the

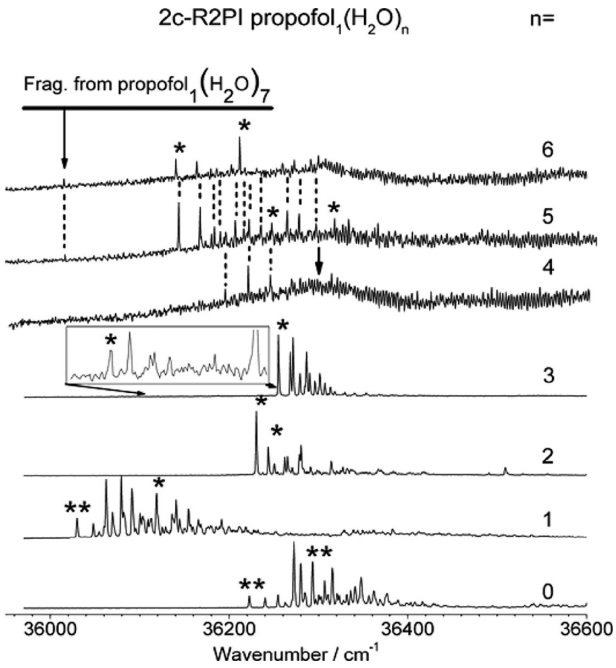

Figure 1. Two-color REMPI of propofol$(H_2O)_{0-6}$ obtained in a expansion of propofol and water in He. The asterisks highlight the position of the 0−0 red-most bands (presumably the 0−0 transitions) of the detected isomers. The arrow marks the wavelength employed to record the propofol$(H_2O)_4$ IR/UV spectrum.

0_0^0 transitions of the isomers found on each stoichiometry. Some species present overlapping transitions, as indicated by the double asterisks. The mass spectrum for a mixture of propofol/water can be found in Figure S2 (Supporting Information). It was demonstrated in previous studies[13] that four conformers are found for the bare molecule but the inclusion of water molecules selectively stabilizes those conformations in which propofol's OH group is less shielded. Furthermore, the water molecules tend to form cyclic structures for the 1:2 and 1:3 clusters. An unusual trend is observed in Figure 1: while well-resolved spectra are obtained for the species containing up to three water molecules, the spectrum of

dx.doi.org/10.1021/jp305795u | J. Phys. Chem. A 2012, 116, 8934−8941

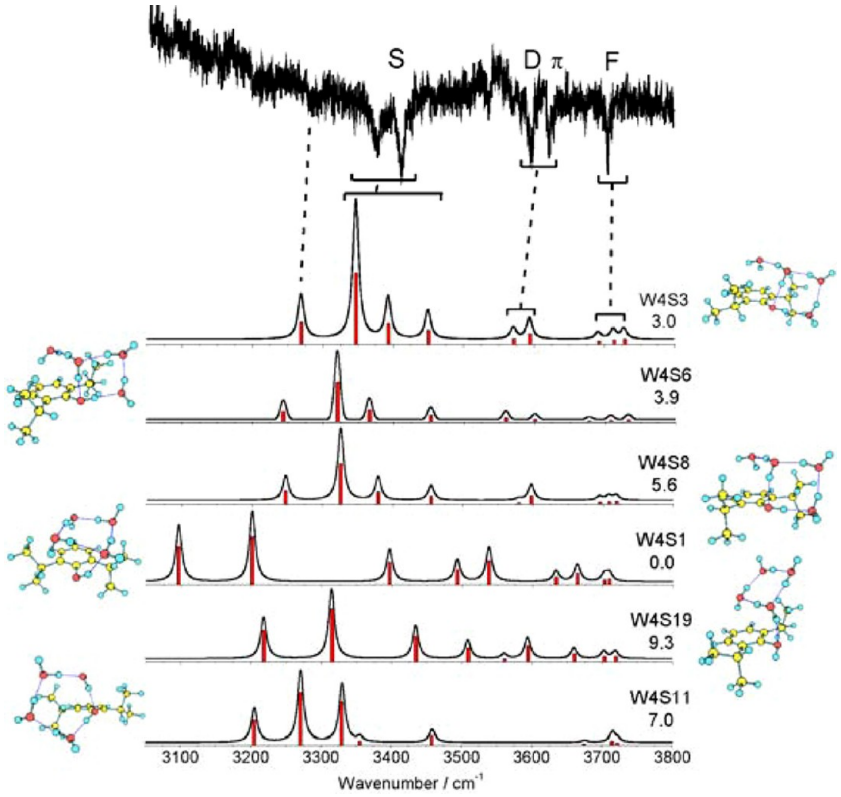

Figure 2. IR/UV spectrum of propofol$(H_2O)_4$ obtained tuning the probe laser to 36 300 cm^{-1}. Some selected calculated structures, together with their simulated spectra, are also shown. The relative stability in kilojoules per mole is shown under each structure's name. A correction factor of 0.938 has been employed to account for vibrational anharmonicity.

propofol$(H_2O)_4$ is a broad absorption. The discrete features that appear in the spectrum are due to fragmentation from higher order clusters (fragmentation is indicated with dashed lines in Figure 1). However, some discrete features are again found in the propofol$(H_2O)_5$ spectrum. The same trend is observed for propofol$(H_2O)_6$, for which a significant reduction in the broad absorption is observed. In addition, several well-resolved strong vibronic bands are observed. Unexpectedly, the spectrum of propofol$(H_2O)_8$ (Figure S3 of the Supporting Information) presents no broad absorption. In the following we will analyze separately the spectroscopy of propofol$(H_2O)_{4-6}$ clusters.

Propofol$(H_2O)_4$. Despite the absence of discrete features in the spectrum of propofol$(H_2O)_4$, it is still possible to record its IR/UV spectrum, setting the UV laser in the spectral region covered by the broad absorption. For example, tuning the probe UV laser at 36 300 cm^{-1} (arrow in Figure 1), the IR/UV spectrum in Figure 2 is obtained. As a further test, an IR/UV spectrum was recorded in the 1:5 and 1:6 mass channels with the probe laser tuned at 36 300 cm^{-1}. Different spectra from that in Figure 2 were obtained, demonstrating that the IR in Figure 2 belongs to propofol$(H_2O)_4$.

The spectrum is composed of several vibronic features built on a broad absorption. The nonexistence of a *window region*, a section of the spectrum between ∼3550 and 3650 cm^{-1} without any spectral feature,[25] indicates that the water molecules are not forming a cyclic structure, but that they are arranged in a more complex way.

Although the signal-to-noise ratio is not as good as for other species (see below), it allows assignment of the cluster by comparison with the calculated structures. Hundreds of structures were found for this cluster using molecular mechanics; 51 were selected for optimization at the M06-2X/6-311++G(d,p) level, resulting in 47 different structures (Figure S4 of the Supporting Information). Although some of the structures differ only in the relative orientation of the water molecules' free OH bonds, making it impossible to carry out a univocal assignment, the structures can be grouped attending to the similarity of their spectra and a final assignment to a group of structures is attainable. For example, in Figure 2 the calculated spectra of W4S3, W4S6, and W4S8, which are members of the same family, are presented, together with ball-and-stick representations of their structures. As can be seen, all three predicted spectra are almost identical, and reproduce reasonably well the experimental trace. Therefore, we assign the propofol$(H_2O)_4$ single detected isomer to a structure of the W4S3 family. Nevertheless, due to the shape of the spectrum, we cannot rule out the existence of other minority isomers hidden in the broad absorption.

Figure 2 also offers a comparison with the spectra from representative structures of other three groups: W4S1, W4S19, and W4S11. The first one is the calculated global minimum. In this structure, the water molecules form a cyclic structure which interacts with the aromatic ring and the OH moiety. W4S19 is relatively similar to W4S1, but in this case propofol acts as proton donor to the ring of waters. Such a difference results in a structure less stable by ∼10 kJ/mol. Finally, W4S11 presents the four water molecules forming a pentagonal structure with propofol's hydroxy group, resembling $(H_2O)_5$ the most stable isomer. However, it is ∼7 kJ/mol above the global minimum. As can be seen, the spectra of these three structures are considerably different from the experimental trace, reinforcing

dx.doi.org/10.1021/jp305795u | J. Phys. Chem. A 2012, 116, 8934−8941

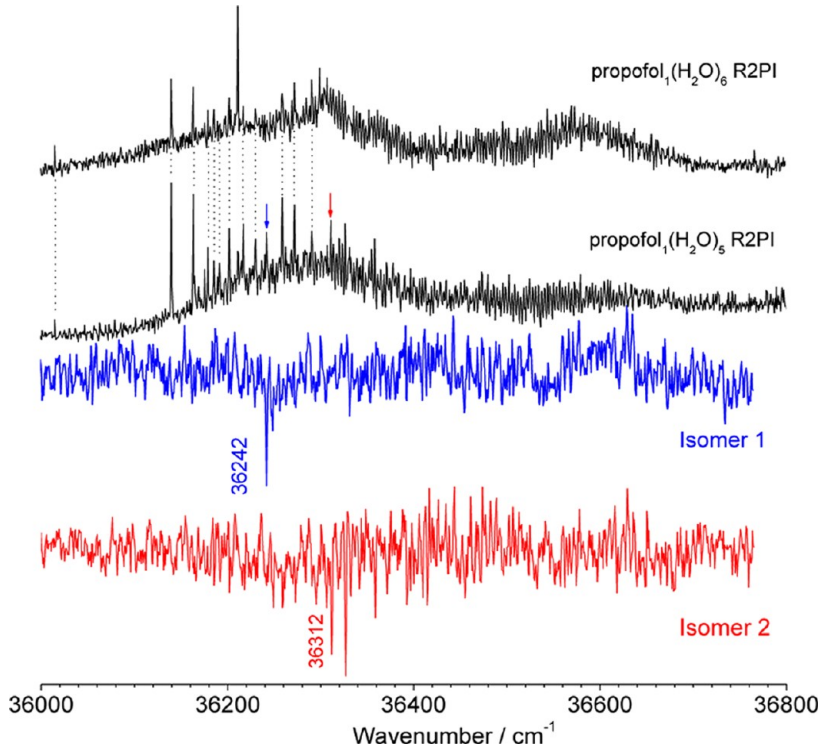

Figure 3. Comparison between the propofol$(H_2O)_5$ UV/UV hole burning obtained probing the transitions at 36 242 and 36 312 cm^{-1}, and the two-color REMPI spectrum. The spectrum of propofol$(H_2O)_6$ is also shown to highlight the existence of fragmentation, indicated by the vertical dotted lines. Two isomers of propofol$(H_2O)_5$ are found.

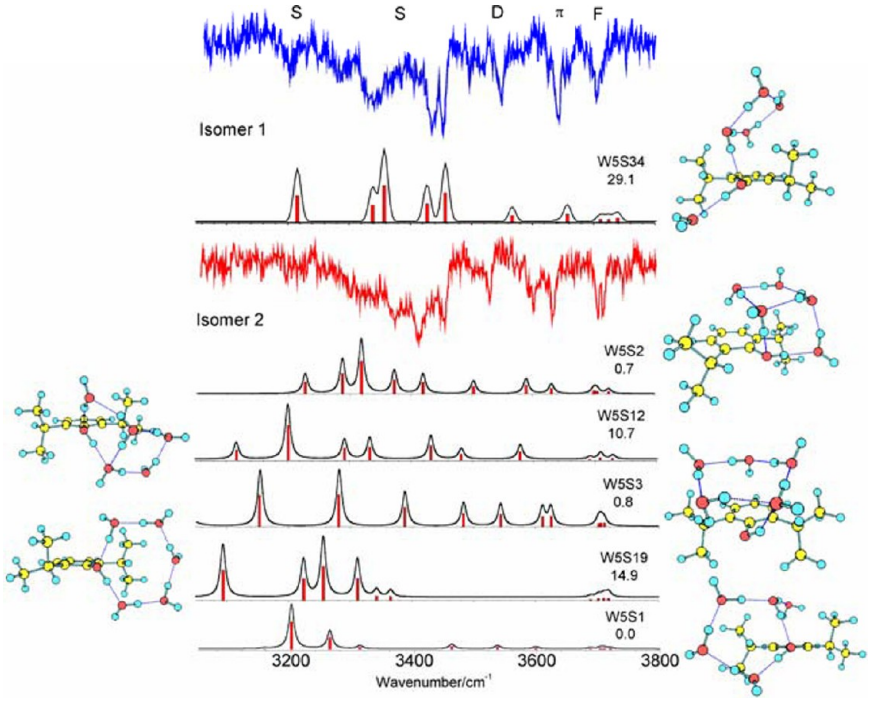

Figure 4. IR/UV spectrum of the two isomers detected for propofol$(H_2O)_5$ obtained probing the transitions at 36 242 and 36 312 cm^{-1}, respectively. Some selected calculated structures, together with their simulated spectra, are also shown. The relative stability in kilojoules per mole is shown under each structure's name. A correction factor of 0.938 has been employed to account for vibrational anharmonicity.

the proposed assignment. The complete set of calculated spectra are collected in Figure S5 of the Supporting Information.

Propofol$(H_2O)_5$. Most of the vibronic transitions present in the spectrum of propofol$(H_2O)_5$ are due to fragmentation from higher order clusters (mainly from propofol$(H_2O)_6$). Nevertheless, two isomers are found using UV/UV hole burning (Figure 3), with band origins at 36 242 and 36 312 cm^{-1}, respectively. None of them exhibits a broad absorption that could correlate with that observed in the REMPI spectrum, and

dx.doi.org/10.1021/jp305795u | J. Phys. Chem. A 2012, 116, 8934−8941

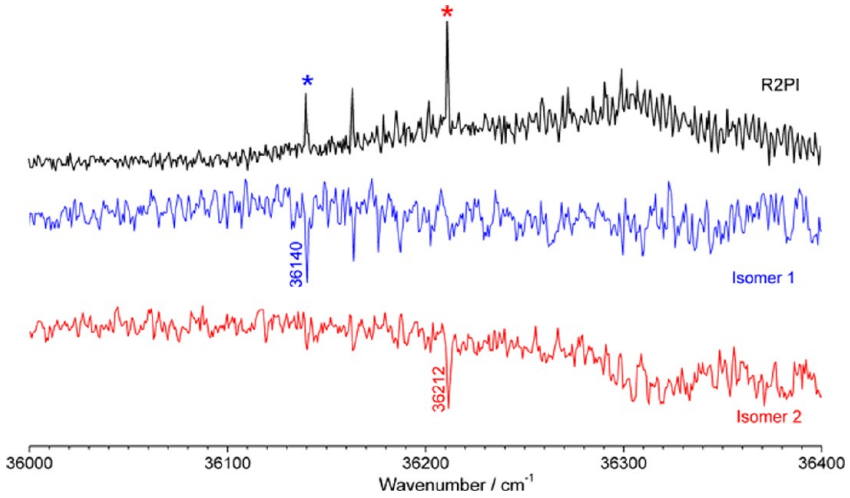

Figure 5. UV/UV hole burning of propofol$(H_2O)_6$ obtained probing the transitions at 36 140 and 36 212 cm^{-1}, respectively. Two isomers are found. The two-color REMPI spectrum is also shown for comparison.

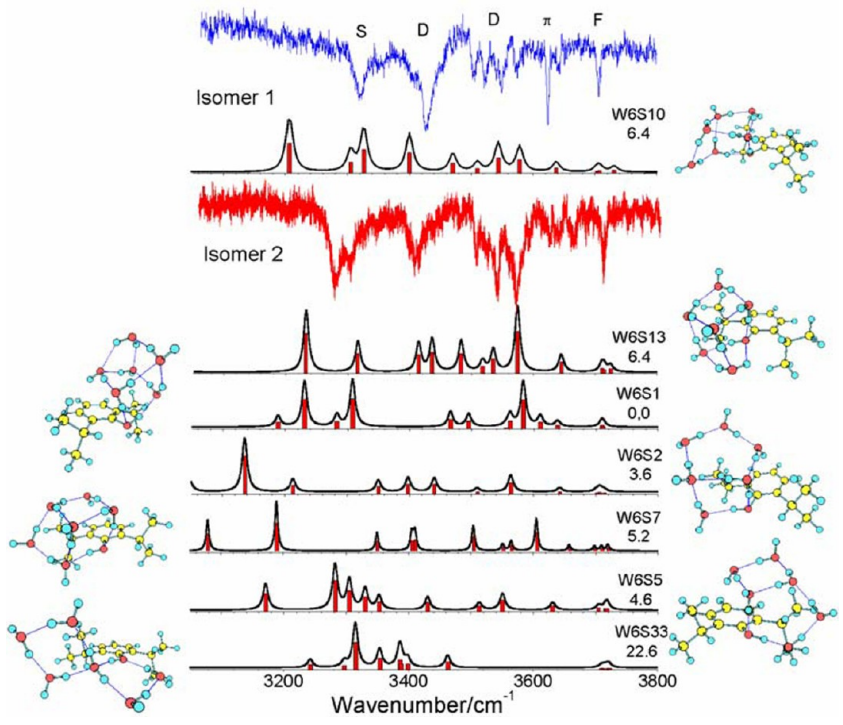

Figure 6. IR/UV spectra of the two isomers detected for propofol$(H_2O)_6$ obtained probing the transitions at 36 140 and 36 212 cm^{-1}, respectively. Some selected calculated structures, together with their simulated spectra, are also shown. The relative stability in kilojoules per mole is shown under each strucutre's name. A correction factor of 0.938 has been employed to account for vibrational anharmonicity.

therefore, the presence of additional isomers cannot be completely ruled out. Several wavelengths were probed in the 36 100−36 800 cm^{-1} interval looking for additional conformers with no success. The IR/UV spectra obtained probing transitions of the detected isomers are collected in Figure 4. Several additional wavelengths were also tested using IR/UV double resonance, but no different spectra were obtained, apart from those in Figure 4. An improvement in the signal-to-noise ratio of the IR/UV trace with respect to the spectrum in Figure 2 is observed. Also, no broad absorption is evident. The spectra in Figure 4 are composed of a considerable number of vibronic transitions, covering the whole range scanned. No laser intensity is obtained below 3100 cm^{-1}, and therefore we cannot rule out the presence of additional bands at longer wavelengths.

Figure 4 also presents some representative calculated structures, together with their simulated spectra. The molecular mechanics exploration yields more than 1000 initial structures, most of them differing slightly in the position of the water molecules. Thirty-eight of such structures were submitted for full optimization using density functional theory (DFT), resulting in the 36 structures collected in Figure S6 of the Supporting Information, while their calculated spectra are collected in Figure S7 of the Supporting Information. The comparison between calculated and experimental spectra leads us to tentatively assign isomer 1 to W5S34 and isomer 2 to

dx.doi.org/10.1021/jp305795u | J. Phys. Chem. A 2012, 116, 8934−8941

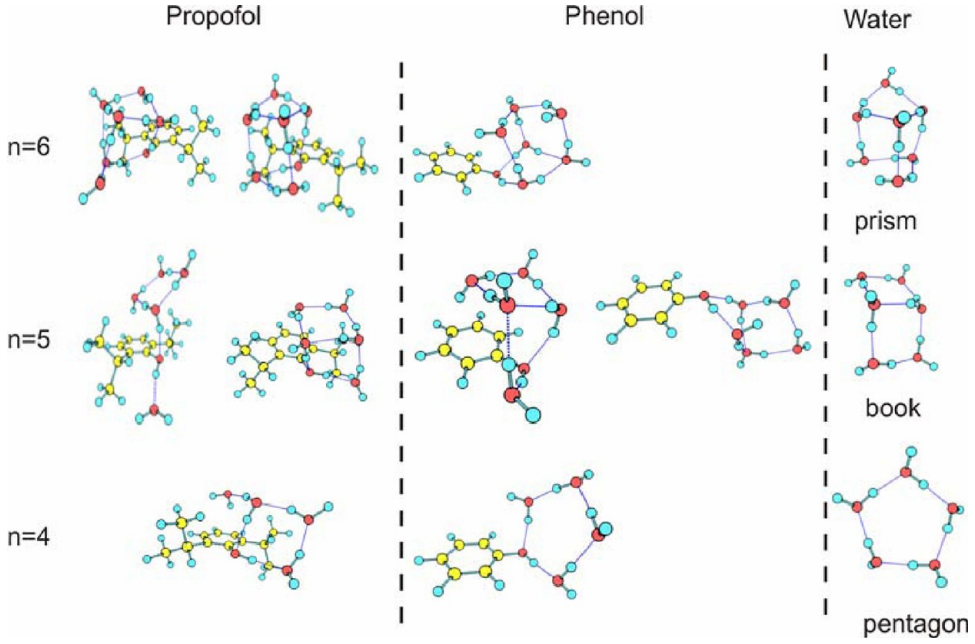

Figure 7. Comparison between the assigned structures in this work and those found for phenol/water clusters and for pure water clusters. The phenol/water clusters were taken from refs 18, 21, and 31 and reoptimized at the M06-2X 6-311++G(d,p)level, while those for pure water clusters were taken from ref 26 and reoptimized at the same calculation level.

W5S2. At first glance the former is somehow an unexpected structure: due to the water high self-aggregation energy, one would expect only structures in which all the water molecules interact. Therefore, such an assignment must be taken with caution. Nevertheless, W5S34 is a combination of the most stable structure observed for propofol$(H_2O)_1$ and a $(H_2O)_4$ cluster,[26] although it is relatively high in energy (~29 kJ/mol above the global minimum). Thus, if the proposed assignment is correct, its anomalously high population in the jet may be a consequence of the cluster formation process.

Isomer 2 is assigned to W5S2, a structure in which the water molecules are forming a book-type structure, which also interacts with the aromatic ring. Such kinds of structures are among the most stable ones for $(H_2O)_6$. It is worthy to note that if the book-type structure is not interacting with the aromatic ring, as in W5S12, the spectrum does not fit the experimental trace.

Once more, the most stable calculated structures, in which the water molecules are forming planar structures, i.e., pentagons (W5S1) or hexagons (W5S3, W5S19), are not detected. The latter structures resemble some of the most stable conformation of $(H_2O)_6$.[26,27]

Propofol$(H_2O)_6$. Several discrete transitions are evident in the spectrum of the 1:6 species, allowing the detection of two isomers using UV/UV hole burning (Figure 5). The IR/UV spectra of the two detected isomers are presented in Figure 6, together with the simulated spectra of several representative structures. The conformational search resulted in ~10 000 structures for this stoichiometry, 42 of which were subjects of further optimization using DFT (Figure S8, Supporting Information). The signal-to-noise ratio of the spectra in Figure 6 is better than for previous species, probably due to the drop in intensity of the background absorption. Comparison with the calculated spectra (Figure 6 and Figure S9 of the Supporting Information) leads us to tentatively assign isomer 1 to W6S10, while isomer 2 is assigned to W6S13. In both structures, the water molecules form a cagelike hydrogen bond network. Such structures resemble very closely the most stable structures of $(H_2O)_7$.[26,28]

Figure 6 also shows other representative structures, together with their calculated spectra. W6S1, the global minimum, has the water molecules forming a prism which presents a direct interaction with the aromatic ring. The water molecules form a chair-type structure in W6S2, which is 3.6 kJ/mol higher in energy. Other possible structures are pseudocubes (W6S7) and bicycles (W6S33); the latter one is relatively high in energy compared with the global minimum, but the rest of the structures presented in Figure 6 are well within the stability window of the species that could be found in the expansion.

DISCUSSION

Cluster Structure: Comparison with Similar Systems. The calculations predict a large number of structures with very similar energies. However, only one isomer is found for the 1:4 cluster and two isomers are detected for the 1:5 and 1:6 species. Such difference between predictions and experiment may be related to the cluster growth process. Formation of, for example, the 1:4 species can proceed in two ways: either water molecules are added sequentially to the chromophore or the collision of a water cluster with the chromophore leads to the final cluster, after evaporation of some solvent molecules. If the latter is the predominant mechanism for the cluster growth, the presence of a limited number of species for each stoichiometry could be due to the difficulty of trapping the cluster of water in a local minimum. As all the water molecules move together, they can more easily find an energetically accessible path to reach the most favorable solvation site.

Such growth could also explain the detection of W5S34, a structure which is relatively high in energy, while other predicted, more stable species are not. W5S34 is the combination of the 1:1 most stable structure and the most stable calculated structure of 1:4. Thus, it may be the result of

dx.doi.org/10.1021/jp305795u | J. Phys. Chem. A 2012, 116, 8934−8941

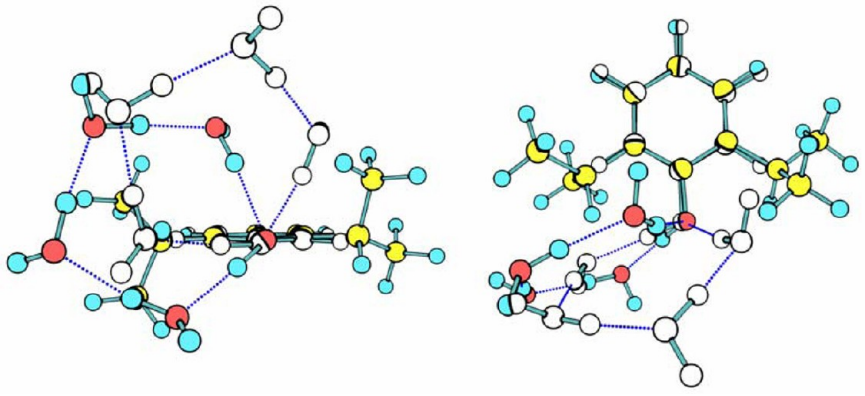

Figure 8. Two views of the superposition of structure W4S11 and the structure assigned in ref 21 to phenol$(H_2O)_4$ and reoptimized at the M06-2X 6-311++G(d,p) level.

the collision of the 1:1 cluster with a $(H_2O)_4$ or even a $(H_2O)_5$ cluster, which loses one of the water molecules.

Figure 7 shows a comparison between the structures assigned in the present work, a set of similar structures for pure water,[26] and those found for phenol−water clusters.[17,29] Perhaps the most striking difference between all three sets of structures is the absence of pentameric structures for propofol$(H_2O)_4$. Certainly, such a structure is by far the most stable found for pure water clusters and was also found in the phenol$(H_2O)_4$ single detected isomer. Figure 8 shows a comparison between propofol$(H_2O)_4$ and phenol$(H_2O)_4$ clusters calculated at the same level of theory. As can be seen, the isopropyl groups force the ring of waters to move aside, while propofol's OH moves out of the plane of the ring. Such displacements may be the reason for the loss of stability of such structure.

Regarding the clusters containing five and six water molecules, despite the presence of the two voluminous hydrophobic groups, the detected structures agree very well with those observed for phenol and with the calculated most stable pure water clusters, with the exception of W5S34, as explained above. Such behavior is at the heart of the hydrophobic effect: the water self-aggregation energy is so high that it is difficult to insert other groups into the water hydrogen-bond networks.

Another important observation is that the transition from (planar) cyclic to (nonplanar) noncyclic structures occurs with six water molecules in pure water clusters and with the fifth water molecule in phenol/water clusters. However, such a transition takes place with four water molecules in propofol, as a consequence of the steric hindrance introduced by the isopropyl groups.

Spectral Shape. A significant change in the REMPI spectral shape with the cluster's size is observed in Figure 1: while well-resolved spectra are obtained for the bare molecule and the clusters containing one to three water molecules, a broad absorption dominates the spectra of those containing four to six water molecules. The cleanliness of the spectrum of the 1:8 species (not shown) indicates that the broad absorption is not due to spectral congestion. A possible explanation is a reduction in the S_1 electronic state lifetime. Figure 9 shows propofol-$(H_2O)_{0-6}$ S_1 lifetime evolution with the number of water molecules, while all the transients together with their best fit are collected in Figure S8 of the Supporting Information (a detailed description of the experimental procedure employed to record the lifetimes may be found in ref 14). As can be seen, the bare molecule presents the shortest excited state lifetime and a

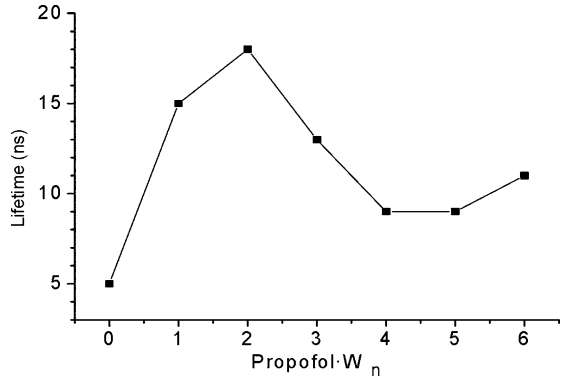

Figure 9. Variation of propofol's S_1 state lifetime with number of water molecules. The lifetime for propofol$(H_2O)_5$ corresponds to the isomer to the red. All the transients recorded together with the best fit are collected in Figure S8 of the Supporting Information.

substantial increase is observed upon complexation. The lifetime becomes more or less constant with the size for clusters containing four water molecules or more. Thus, the observed lifetimes are excluded as being responsible for the broad absorption.

Another likely explanation is the flexibility of the cluster's structure: a floppy structure may experience large conformational changes upon excitation. Certainly, W4S3, the structure assigned to propofol$(H_2O)_4$, has a water molecule floating over the aromatic ring. Such a water molecule may experience a large displacement upon excitation due to the expansion of the electronic cloud. Such an effect has been observed for other aromatic−water systems.[30]

The two structures found for propofol$(H_2O)_5$ are also very dynamic and are expected to experience large-amplitude movements upon excitation. Accordingly, the observed spectrum is mainly a broad absorption with only two discrete features due to the complex and some additional features due to fragmentation from higher order clusters. The increasing rigidity of the structures of the detected propofol$(H_2O)_6$ clusters results in a noticeable reduction of the broad absorption and in the appearance of some discrete bands.

■ CONCLUSIONS

In the present work, the laser spectroscopy of propofol solvated by four to six water molecules is analyzed. The two-color REMPI spectrum of propofol$(H_2O)_4$ consists of a broad

dx.doi.org/10.1021/jp305795u | J. Phys. Chem. A 2012, 116, 8934−8941

absorption with no discrete features. Using IR/UV spectroscopy, it is possible to obtain the spectrum of a single isomer, assigned to a structure in which three water molecules form an eight-member ring with propofol's hydroxy moiety, while the fourth water molecule interacts both with the aromatic ring and with the ring of waters. Such a structure is very dynamic and will experiment large structure changes upon ionization. This may well be the reason for the absence of discrete features in the spectrum.

The REMPI spectrum of the cluster containing five water molecules presents some discrete features, built on top of a broad absorption. Two isomers were found using UV/UV hole burning, and their IR spectra were recorded using IR/UV double resonance spectroscopy. The isomer with the origin to the red is assigned to a structure which resembles the propofol$(H_2O)_1$ most stable isomer interacting with an $(H_2O)_4$ cluster. Nevertheless, such an assignment must be made with caution: this calculated isomer is relatively high in energy (29.1 kJ/mol above the global minimum) but it may be favored by the cluster formation mechanism. On the other hand, the water molecules form a book structure in the second propofol$(H_2O)_5$ cluster, which is one of the most stable structures of $(H_2O)_6$.

Two isomers are also found for propofol$(H_2O)_6$, assigned to clusters with water in cage and prism conformations, which are also the two most stable $(H_2O)_7$ water conformers. Such structures are less flexible than those found for the 1:4 and 1:5 clusters. Thus, there seems to be a correlation between structure flexibility and the absence of resolved features in the REMPI spectrum.

Comparison with phenol−water clusters shows that the isopropyl groups influence the conformations that the water hydrogen bond networks can adopt, but they cannot completely block the access of water to propofol's hydroxy group. Still, they are able to force water to adopt noncyclic structures for a relatively small cluster size. A tendency of water to form structures which resemble those calculated for pure water clusters is observed, due to water's high self-aggregation energy.

■ ASSOCIATED CONTENT

Supporting Information

Complete set of calculated structures, together with their calculated spectra, S_1 electronic state transients, and Cartesian coordinates for the assigned isomers. This material is available free of charge via the Internet at http://pubs.acs.org.

■ AUTHOR INFORMATION

Corresponding Author

*E-mail: josea.fernandez@ehu.es. Phone: +34-946-015387. Fax: +34-946-013500.

Notes

The authors declare no competing financial interest.

■ ACKNOWLEDGMENTS

The research leading to these results has received funding from the Spanish Ministry of Science and Innovation-MICINN (Consolider-Ingenio 2010/CSD2007-00013 and CTQ2009-14364). I.L. would like to thank the GV for a predoctoral fellowship. Computational resources from the SGI/IZO-SGIker and i2BASQUE were used for this work. Technical and human support provided by the Laser Facility of the SGIker (UPV/EHU, MICINN, GV/EJ, ESF) is also gratefully acknowledged.

■ REFERENCES

(1) Schermann, J. P. *Spectrocopy and Modelling of Biomolecular Building Blocks*; 1st ed.; Elsevier: Amsterdam, 2008.
(2) Hobza, P.; Muller-Dethlefs, K. *Non-Covalent Interactions*; RCS Publishing: London, 2010.
(3) Pribble, R. N.; Zwier, T. S.. *Science* **1994**, *265*, 75−79.
(4) Baquero, E. E.; James, W. H.; Choi, S. H.; Gellman, S. H.; Zwier, T. S. *J. Am. Chem. Soc.* **2008**, *130*, 4784−4794.
(5) Schwing, K.; Fricke, H.; Bartl, K.; Polkowska, J.; Schrader, T.; Gerhards, M.. *ChemPhysChem* **2012**, *13*, 1576−1582.
(6) Cocinero, E. J.; Gamblin, D. P.; Davis, B. G.; Simons, J. P. *J. Am. Chem. Soc.* **2009**, *131*, 11117−11123.
(7) Cocinero, E. J.; Stanca-Kaposta, E. C.; Dethlefsen, M.; Liu, B.; Gamblin, D. P.; Davis, B. G.; Simons, J. P. *Chem.—Eur. J.* **2009**, *15*, 13427−13434.
(8) Plutzer, C.; Hunig, I.; Kleinermanns, K.; Nir, E.; de Vries, M. *ChemPhysChem* **2003**, *4*, 838−842.
(9) Nir, E.; Janzen, C.; Imhof, P.; Kleinermanns, K.; de Vries, M. S. *Phys. Chem. Chem. Phys.* **2002**, *4*, 732−739.
(10) Aguado, E.; León, I.; Cocinero, E. J.; Lesarri, A.; Fernández, J. A.; Castaño, F. *Phys. Chem. Chem. Phys.* **2009**, *11*, 11608−11616.
(11) León, I.; Aguado, E.; Lesarri, A.; Fernández, J. A.; Castaño, F. *J. Phys. Chem. A* **2009**, *113*, 982−988.
(12) Lesarri, A.; Shipman, S. T.; Neill, J. L.; Brown, G. G.; Suenram, R. D.; Kang, L.; Caminati, W.; Pate, B. H. *J. Am. Chem. Soc.* **2010**, *132*, 13417−13424.
(13) León, I.; Cocinero, E.; Millán, J.; Jaeqx, S.; Rijs, A.; Lesarri, A.; Castaño, F.; Fernández, J. A. *Phys. Chem. Chem. Phys.* **2012**, *14*, 4398.
(14) León, I.; Millán, J.; Cocinero, E.; Lesarri, A.; Castaño, F.; Fernández, J. A. *Phys. Chem. Chem. Phys.* **2012**, *14*, 8956−8963.
(15) León, I.; Cocinero, E. J.; Millán, J.; Rijs, A. M.; Usabiaga, I.; Lesarri, A.; Castaño, F.; Fernández, J. A. *J. Chem. Phys.* **2012**, *137*, 074303, DOI: 10.1063/1.4743960.
(16) Fredericks, S. Y.; Pedulla, J. M.; Jordan, K. D.; Zwier, T. S. *Theor. Chem. Acc.* **1997**, *96*, 51−55.
(17) Roth, W.; Schmitt, M.; Jacoby, C.; Spangenberg, D.; Janzen, C.; Kleinermanns, K. *Chem. Phys.* **1998**, *239*, 1−9.
(18) Jacoby, C.; Roth, W.; Schmitt, M.; Janzen, C.; Spangenberg, D.; Kleinermanns, K. *J. Phys. Chem. A* **1998**, *102*, 4471−4480.
(19) Kleinermanns, K.; Janzen, C.; Spangenberg, D.; Gerhards, M. *J. Phys. Chem. A* **1999**, *103*, 5232−5239.
(20) Janzen, C.; Spangenberg, D.; Roth, W.; Kleinermanns, K. *J. Chem. Phys.* **1999**, *110*, 9898−9907.
(21) Luchow, A.; Spangenberg, D.; Janzen, C.; Jansen, A.; Gerhards, M.; Kleinermanns, K. *Phys. Chem. Chem. Phys.* **2001**, *3*, 2771−2780.
(22) *Maestro*, version 9.2; *Macromodel*, version 9.5.207; Schrödinger, Inc.: New York, 2010.
(23) *Gaussian 09*, rev. A02; Gaussian, Inc.: Wallingford, CT, 2009.
(24) Boys, S. F.; Bernardi, F. *Mol. Phys.* **1970**, *19*, 553−566.
(25) Mikami, N. *Bull. Chem. Soc. Jpn.* **1995**, *68*, 683−695.
(26) Shields, R. M.; Temelso, B.; Archer, K. A.; Morrell, T. E.; Shields, G. C. *J. Phys. Chem. A* **2010**, *114*, 11725−11737.
(27) Pérez, C.; Muckle, M. T.; Zaleski, D. P.; Seifert, N. A.; Temelso, B.; Shields, G. C.; Kisiel, Z.; Pate, B. H. *Science* **2012**, *336*, 897−901.
(28) Pérez, C.; Muckle, M. T.; Zaleski, D. P.; Seifert, N. A.; Pate, B. H. Presented at the 67th OSU International Symposium on Molecular Spectroscopy (Columbus, OH), 2012; Commun. RH02.
(29) Schmitt, M.; Jacoby, C.; Gerhards, M.; Unterberg, C.; Roth, W.; Kleinermanns, K. *J. Chem. Phys.* **2000**, *113*, 2995−3001.
(30) Pribble, R. N.; Garrett, A. W.; Haber, K.; Zwier, T. S. *J. Chem. Phys.* **1995**, *103*, 531−544.
(31) Ebata, T.; Fujii, A.; Mikami, N. *Int. J. Mass Spectrom. Ion Processes* **1996**, *159*, 111−124.